Chalmers Publication Library

(Article begins on next page)

Influence of Fiber-Bragg Grating-Induced Group-Delay Ripple in High-Speed Transmission Systems

Ekawit Tipsuwannakul, Jianqiang Li, Tobias A. Eriksson, Lars Egnell, Fredrik Sjöström, Johan Pejnefors, Peter A. Andrekson, and Magnus Karlsson

***Abstract*—The implementation of a chirped fiber-Bragg grating (FBG) for dispersion compensation in high-speed (up to 120 Gbit/s) transmission systems with differential and coherent detection is, for the first time, experimentally investigated. For systems with differential detection, we examine the influence of group-delay ripple (GDR) in 40 GBd 2-, 4-, and 8-ary differential phase shift keying (DPSK) systems. Furthermore, we conduct a nonlinear-tolerance comparison between the systems implementing dispersion-compensating fibers and FBG modules, using a 5×80 Gbit/s 100-GHz-spaced wavelength division multiplexing 4-ary DPSK signal. The results show that the FBG-based system provides a 2 dB higher optimal launch power, which leads to more than 3 dB optical signal-to-noise ratio (OSNR) improvement at the receiver. For systems with coherent detection, we evaluate the influence of GDR in a 112 Gbit/s dual-polarization quadrature phase shift keying system with respect to signal wavelength. In addition, we demonstrate that, at the optimal launch power, the 112 Gbit/s systems implementing FBG modules and that using electronic dispersion compensation provide similar performance after 840 km transmission despite the fact that the FBG-based system delivers lower OSNR at the receiver. Lastly, we quantify the GDR mitigation capability of a digital linear equalizer in the 112 Gbit/s coherent systems with respect to the equalizer tap number (N_{tap}). The results indicate that at least $N_{tap} = 9$ is required to confine Q-factor variation within 1 dB.**

***Index Terms*—Coherent detection; Differential detection; Dispersion compensation; Equalization; Fiber Bragg grating; Group delay ripple; Phase shift keying.**

I. INTRODUCTION

Fiber-Bragg grating (FBG)-based dispersion-compensating modules exhibit several attractive characteristics, e.g., compact size, low insertion loss, negligible latency, and the absence of nonlinearities. This has resulted in the modules being deployed in 10 Gbit/s transmission systems as an alternative to dispersion-compensating fibers (DCFs). However, due to imperfections in the fabrication process, FBG modules give rise to group-delay ripple (GDR), which can

cause signal distortion [1–5]. This raises concerns with regard to practical implementations of such devices in transmission systems with bit-rates (per channel) beyond 10 Gbit/s.

In recent years, the influence of FBG-induced GDR in higher than 10 Gbit/s systems with direct or differential detection has been extensively investigated by means of simulations with respect to various modulation formats, for instance, on/off keying (OOK), differential phase shift keying (DSPK), and return-to-zero (RZ) [2,3,6]. A similar investigation of a 40 Gbit/s binary DPSK system has also been experimentally conducted as a function of the GDR presented in the system [4]. In addition, successful transmission of 10 Gbit/s OOK and 43 Gbit/s 4-ary DPSK (DQPSK) with inline FBG modules over 1000 km has recently been reported [7,8]. These results show the feasibility of using FBG modules for dispersion compensation in high-speed transmission systems. However, the highest bit-rate previously reported is still limited to approximately 40 Gbit/s. Furthermore, the benefit of the device's lack of nonlinearity has not been addressed in previous work.

The GDR-induced performance degradation in coherent-detection systems, on the other hand, may be seen as less of a problem since such an impairment can be mitigated to large extent through digital signal processing (DSP), i.e., a linear equalizer. This mitigation capability has been numerically analyzed in [9] and has been shown to be independent of the signal bit-rate. Thus, the use of FBG modules in coherent-detection systems can be very beneficial as it significantly helps in reducing the receiver's complexity, chip area, and power consumption when compared to systems implementing electronic dispersion compensation (EDC). However, this conjecture still lacks experimental support.

In this paper, we experimentally evaluate the feasibility of implementing FBG modules for dispersion compensation in high-speed (up to 120 Gbit/s) transmission systems. The evaluations are performed with respect to the following two aspects.

Firstly, we investigate the performance degradation caused by FBG-induced GDR in differential- and coherent-detection systems. For differential-detection systems, we extend the previous studies by, for the first time, quantifying the GDR-induced penalty in 40 GBd RZ M-ary DPSK ($M = 2, 4, 8$) systems as a function of the number of FBG modules used in the link. Next, we present the first nonlinear-tolerance comparison between the systems implementing DCFs and FBG modules with respect to the optimal launch power (P_L), using $5 \times$ 80 Gbit/s 100-GHz-spaced RZ-DQPSK over a 480 km standard
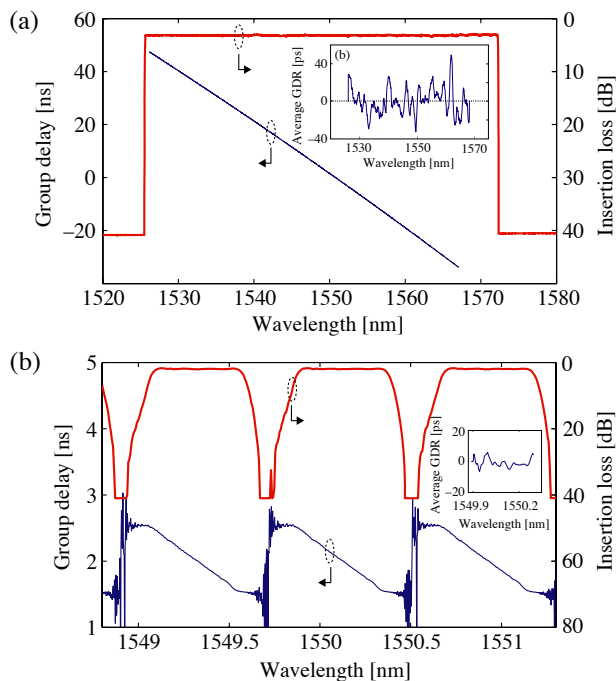
Fig. 1. (Color online) Measured group delay (thin lines) and insertion loss (thick lines) of (a) continuous and (b) 100-GHz-spaced channelized FBG modules, including averaged GDR over 28 GHz bandwidth (insets).

Fig. 2. (Color online) The GDR histograms of (a)–(d) four individual 120 km continuous modules and (e) a concatenation of 8 (5 × 120 km + 3 × 80 km) continuous modules.

single-mode fiber (SMF) link. For coherent-detection systems, we experimentally evaluate the performance of a 112 Gbit/s dual-polarization (DP) quadrature phase shift keying (QPSK) signal after transmission through a concatenation of FBG modules with respect to signal wavelength. The first direct performance comparison between the systems using EDC and FBG modules is also demonstrated over an 840 km SMF link.

Secondly, we assess the GDR mitigation capability in the 112 Gbit/s DP-QPSK coherent-detection system by means of experiments. The mitigation capability investigated here is quantified in the form of Q-factor variations of the signal over a 20 nm wavelength range with respect to the linear equalizer's tap number (N_{tap}). To our knowledge, this is also the first experimental assessment of GDR mitigation capability ever reported.

This paper is organized as follows. Section II provides the properties of the FBG modules used in the experiments. Section III describes the experimental setups of both differential- and coherent-detection systems. Section IV concerns the GDR-induced performance degradation in high-speed transmission systems with differential and coherent detection. Lastly, Section V deals with the GDR mitigation capability of a linear equalizer in coherent systems.

II. PROPERTIES OF THE FBG MODULES UNDER INVESTIGATION

Two types of commercially available FBG modules, namely, continuous and 100-GHz-spaced channelized modules, are investigated in this work. For the continuous modules, there exist two different versions, i.e., 80 km and 120 km continuous
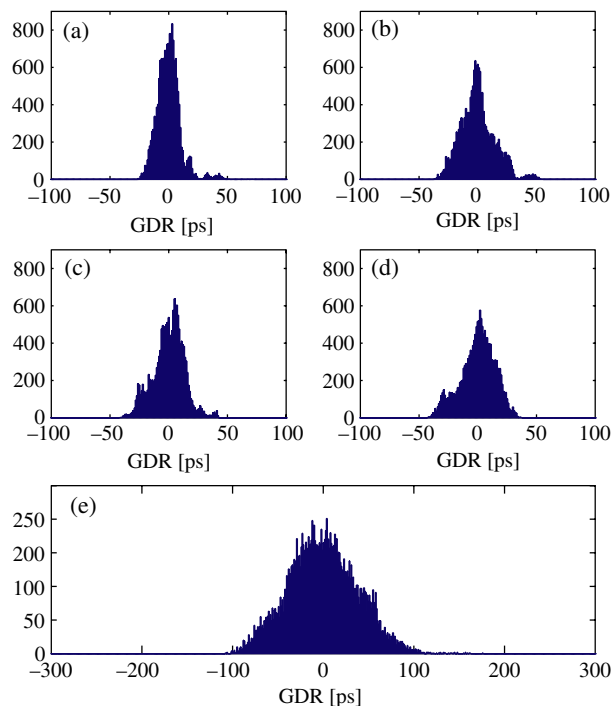
modules. The 80 km modules exhibit dispersion and slope of -1334 ps/nm and -0.46 ps/nm^2 at 1550 nm wavelength, which are opposite to those found in typical 80 km SMFs, ensuring full dispersion compensation for all WDM channels. Similarly, the dispersion and slope present in the 120 km modules are measured to be -2000 ps/nm and -0.69 ps/nm^2, which are opposite to those of typical 120 km SMFs. For the channelized modules, the dispersion present in each WDM channel is opposite to those of typical 120 km SMFs.

The operating wavelengths of both continuous and channelized modules cover the entire C-band. The channelized modules also provide a channel 3 dB bandwidth of 55 GHz and more than 40 dB channel isolation. Figure 1 illustrates the measured group delay and the insertion loss of both 120 km continuous and 120 km channelized modules. By subtracting the group delay with its 2$^{\text{nd}}$-order polynomial fit, the GDR can clearly be observed, as depicted in Fig. 1 (insets). Note that a linear fit was used in the case of the channelized module as dispersion can be considered constant over a narrow bandwidth. In Fig. 2, the GDR histograms of four individual 120 km continuous modules and a concatenation of 8 (5 × 120 km + 3 × 80 km) continuous modules are shown.

The properties of the FBG modules are listed in Table I in comparison to those of the DCFs used Section IV. In addition to the absence of nonlinearities, the notable feature of FBG modules is low insertion loss.

III. THE EXPERIMENTAL SETUP

In this section, the experimental setups of the systems with differential and coherent detection are described.

TABLE I
PROPERTIES OF THE FBG MODULES AND DCFS FOR 120 km SMF

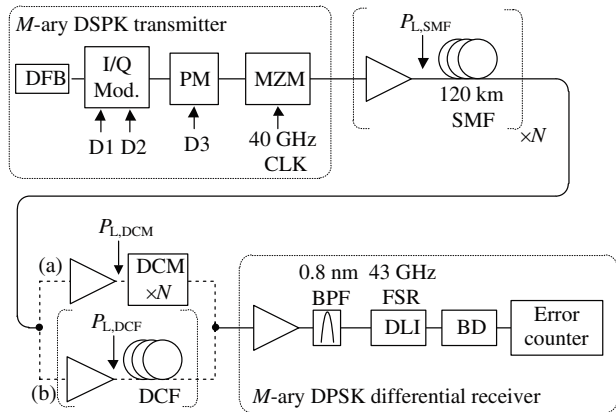| Properties | FBG modules | | | |
| | Continuous | | Channelized | |
	80 km	120 km	120 km	DCF
Insertion loss (α) [dB]	2	3	3	18
Length [km]				18
Dispersion (D) [ps/nm]	−1334	−2000	−2000	−2000
FOM[a] [ps/(nm·dB)]	666	666	666	111

Notes.
[a] Figure of merit $= |D|/\alpha$.

Fig. 3. The experimental setup of 40 GBd *M*-ary RZ-DPSK (*M* = 2, 4, 8) systems with differential detection. Acronyms are given in the text.

Fig. 4. The experimental setup of a 112 Gbit/s DP-QPSK system with coherent detection and a DSP flowchart.

A. Differential-Detection Systems

Figure 3 shows a schematic of 40 GBd *M*-ary RZ-DPSK (*M* = 2, 4, 8) systems with differential detection. As seen, the *M*-ary RZ-DPSK transmitter consisted of a distributed feedback (DFB) laser operating at 1553.12 nm, an inphase/quadrature (I/Q) modulator, a phase modulator (PM), and a Mach–Zehnder modulator (MZM). The I/Q modulator was driven by two 40 Gbit/s binary data streams (D1 and D2), providing an 80 Gbit/s DQPSK signal at the output. The following PM was driven by a third 40 Gbit/s binary data stream (D3), creating a $\pi/4$ phase shift onto DQPSK for 8-ary DPSK generation. The signal was then fed into the MZM driven by a 40 GHz sinusoid to generate an RZ format with 50% duty cycle. All data streams (D1, D2, and D3) were decorrelated pseudo-random binary sequences (PRBSs) with lengths of $2^{11} - 1$. The length of the PRBS was essentially limited by the programming capability of an error counter due to the lack of a pre-coder. In addition, this transmitter can generate 4- and 2-ary DPSK signals by turning off D3 and D2–D3, respectively.

Next, the transmission link was realized by multiple spans of an erbium-doped fiber amplifier (EDFA) followed by a 120 km SMF. The accumulated dispersion was then post-compensated by either a concatenation of 120 km continuous FBG modules or multiple spans of an EDFA and DCF with 18 dB per-span loss on average. It should be noted that the influence of fiber nonlinearities may differ, depending on the dispersion map of the transmission link. A post-compensation
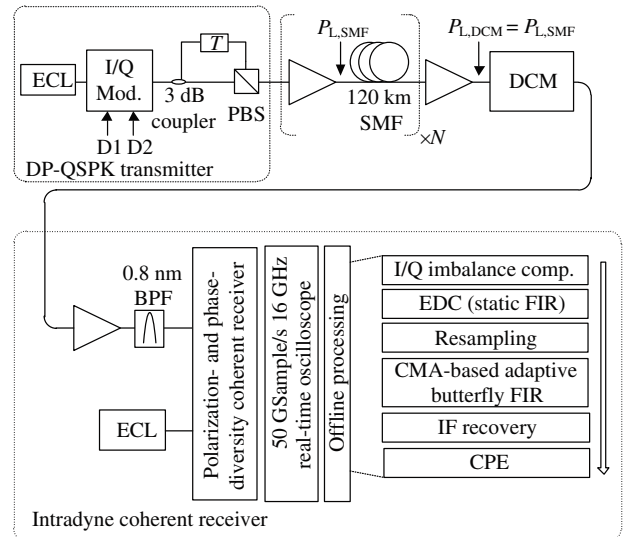
link was chosen in this work as it is expected to provide fewer nonlinear impairments for high-speed signals (≥40 Gbit/s) [10].

At the receiver, the received signal first passed through an optical bandpass filter (BPF) with a 3 dB bandwidth of 100 GHz for noise suppression and differentially demodulated by a delay line interferometer (DLI) with a free spectral range (FSR) of 43 GHz. The demodulated signals were then detected by a balanced detector (BD) and fed into the error counter, which was programmed with the expected differentially demodulated bit patterns. Note that the use of the DLI with a non-ideal FSR can cause performance degradation. However, such degradation has been shown to be negligible when the FSR differs by less than 10% from the ideal value as in this work [11].

B. Coherent-Detection Systems

As illustrated in Fig. 4, a QPSK transmitter consisting of an external cavity laser (ECL) with a linewidth of 500 kHz and an I/Q modulator was used. The modulator was driven by two 28 Gbit/s PRBSs (D1 and D2), with lengths and relative delays of $2^{15} - 1$ and 16,381 bits, respectively. The QPSK signal was then polarization multiplexed through a 3 dB coupler, an optical delay line, and a polarization beam splitter (PBS).

Next, the DP-QPSK signal was launched into a transmission link, comprising multiple spans of a 120 km SMF with an EDFA located upfront followed by concatenation FBG modules for dispersion compensation, and was detected by a conventional coherent receiver. The receiver was made of an 0.8 nm BPF, a free-running ECL with a linewidth of 100 kHz as local oscillator (LO), two PBSs, and two optical 90° hybrids with four integrated BDs. The signal components (I_x, Q_x, I_y, Q_y) from the four BDs were then asynchronously sampled and digitized by a 50 GSample/s real-time oscilloscope with an analog bandwidth of 16 GHz. The four digitized streams, each with 2×10^6 discrete samples, were processed offline.

The DSP started with I/Q imbalance compensation, a static time-domain finite impulse response (FIR) filter for dispersion compensation, and signal resampling. The resampled signal was then polarization demultiplexed and linearly equalized by an N_{tap} $T/2$-spaced adaptive butterfly FIR filter optimized with the standard constant modulus algorithm (CMA). An intermediate-frequency (IF) recovery and carrier-phase estimation (CPE) were subsequently performed using a fast Fourier transform (FFT) method and the 4th-power Viterbi–Viterbi algorithm, respectively. Lastly, BER counting was performed, based on differential-coded symbol-to-bit mapping.

IV. GDR-Induced Performance Degradation in High-Speed Transmission Systems

In this section, we investigate the influence of FBG-induced GDR in high-speed transmission systems with differential and coherent detection. For the differential-detection system, we first compare the GDR-induced penalty among M-ary RZ-DPSK ($M = 2, 4, 8$) at symbol rates of 10 and 40 GBd with respect to the number of continuous FBG modules used in the systems. We then perform the nonlinear-tolerance comparison between the systems implementing DCFs and FBG modules for dispersion compensation, using 5×80 Gbit/s 100-GHz-spaced WDM RZ-DQPSK over the 480 km link.

For coherent-detection systems, we first discuss the influence of GDR induced by both continuous and channelized FBG modules on a 112 Gbit/s DP-QPSK signal with respect to signal wavelengths. We then present the performance comparison between the systems implementing the EDC and FBG modules for dispersion compensation over an 840 km straight-line SMF link.

A. System With Differential Detection

The comparison of the GDR-induced penalty among M-ary RZ-DPSK ($M = 2, 4, 8$) systems was performed with respect to the number of 120-km continuous FBG modules implemented in the link (see Fig. 3(a)). The penalty here is quantified as the required optical signal-to-noise ratio (OSNR) for BER = 10^{-3} relative to the back-to-back sensitivity. In the transmission link, the P_L into the SMF ($P_{L,SMF}$) for each span was adjusted to be 0 dBm to avoid the influence of fiber nonlinearities. The results for the 10 GBd (broken lines) and 40 GBd (solid lines) systems are plotted in Fig. 5. For the 10 GBd
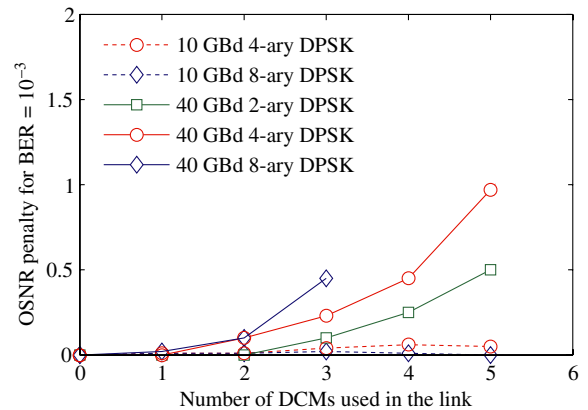

Fig. 5. (Color online) OSNR penalty for BER = 10^{-3} of 10 GBd (broken lines) and 40 GBd (solid lines) M-ary RZ-DPSK signals as a function of transmission distances with (up to) five 120 km continuous FBG modules for dispersion compensation.

systems, we observe no significant penalty after transmission through a concatenation of 5×120 km continuous modules. However, given the same amount of GDR, this penalty becomes significant for the 40 GBd signals. In addition, the results show that the GDR-induced penalty increases with the number of modulation levels and FBG modules used in the link. Notice that since $P_{L,SMF}$ was kept low at 0 dBm, the number of FBG modules used in the case of 40 GBd 8-ary DPSK was limited to 3 modules due to insufficient OSNR at the receiver.

For the nonlinear-tolerance comparison between the systems implementing DCFs and FBG modules, 4 spans of 120 km SMF followed by either a concatenation of 4×120 km continuous FBG modules (see Fig. 3(a)) or 4 spans of DCF (Fig. 3(b)) were used as a transmission link. The signal used in this comparison was 5×80 Gbit/s 100-GHz-spaced RZ-DQPSK, of which the odd and even channels were generated from two independent DQPSK transmitters. Figure 6 plots BER performances (center channel only) of the two investigated systems with respect to the delivered OSNR at the receiver. In the plots, each group of measured data connected with a solid line represents one value of the $P_{L,SMF}$ which was varied from 3 dBm to 14 dBm with 1 dB resolution. For each $P_{L,SMF}$, the P_L into the DCF ($P_{L,DCF}$) and the P_L into the FBG modules ($P_{L,FBG}$) were varied independently to achieve the optimal performance.

As seen in Fig. 6(a), we observe that the transmission performance in a linear regime (low launch powers) of the FBG-based system is penalized by 0.5 dB with respect to the back-to-back performance (broken line), which we attribute to the FBG-induced GDR. Note that this linear penalty may vary depending on the amount of GDR present in the system. Next, for each $P_{L,SMF}$ (solid lines) we see no nonlinear distortion of the signal when increasing $P_{L,FBG}$ (from 8 dBm to 16 dBm with 2 dB resolution) since nonlinearities are absent in the FBG modules. Lastly, by independently optimizing $P_{L,SMF}$ and $P_{L,FBG}$, we find that the optimal performance of the FBG-based system is obtained at $P_{L,SMF}$ = 12 dBm and $P_{L,FBG}$ = 16 dBm, respectively. Note that $P_{L,FBG}$ is limited to 16 dBm due to EDFA saturation.

For the DCF-based system (Fig. 6(b)), on the other hand, we observe that the transmission performance in a linear regime
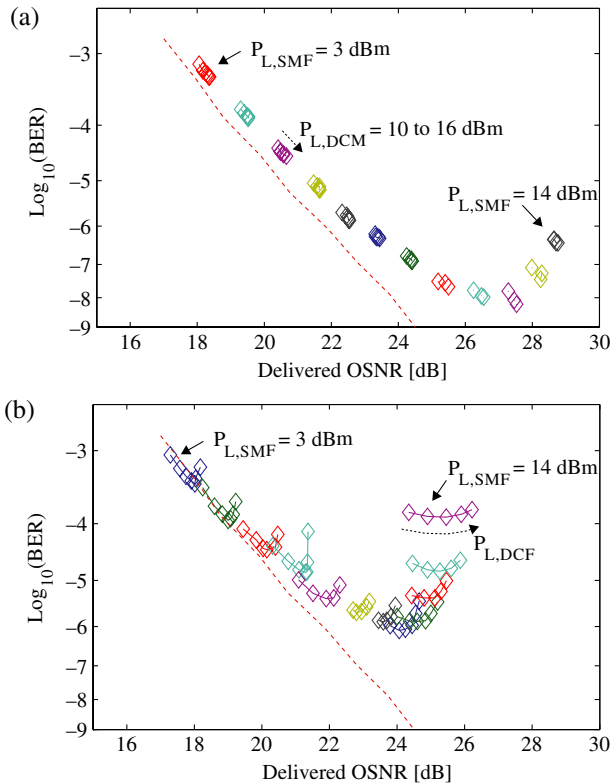
(a)

(b)

Fig. 6.   (Color online) BER performances (center channel only) of 5 × 80 Gbit/s 100-GHz-spaced WDM RZ-DQPSK signals as a function of delivered OSNR over 480 km SMFs with (a) FBG modules and (b) DCFs for dispersion compensation. The broken lines represent the back-to-back BER performance of the WDM signals (center channel).

is consistent with the back-to-back performance (broken line). We also find that, by sweeping $P_{\mathrm{L,DCF}}$ (in the 8 dB range around its optimal point with 2 dB resolution), the curve (solid line) exhibits an optimal value, which is a compromise between noise and fiber nonlinearities. This is indeed attributed to certain OSNR degradation at the receiver as $P_{\mathrm{L,DCF}}$ must be reduced to avoid a strong nonlinear interaction. In addition, to minimize the overall nonlinear distortion of the entire system, we find that the optimal $P_{\mathrm{L,SMF}}$ is less than that of the FBG-based system. As a result, the optimal performance of the DCF-based system is found to be at $P_{\mathrm{L,SMF}} = 10$ dBm and $P_{\mathrm{L,DCF}} = 6$ dBm. As seen, using FBG modules instead of DCFs provides 2 dB improvement of the optimal $P_{\mathrm{L,SMF}}$, which (together with $P_{\mathrm{L,FBG}} = 16$ dBm) leads to more than 3 dB higher OSNR at the receiver. It should be noted that the insertion loss of the DCFs used in this work is two times larger than that of current commercial products. However, as most of the ASE noise is generated by EDFAs with higher gain (i.e., those located in the SMF spans), similar conclusions are still expected when using low-loss DCFs in the comparison.

B. Systems With Coherent Detection

The performance degradation caused by a concatenation of 100-GHz-spaced channelized FBG modules was first evaluated with the CMA equalizer $N_{\mathrm{tap}} = 15$. During these
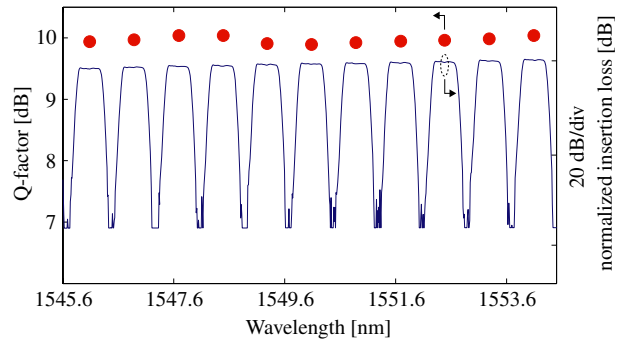

Fig. 7.   (Color online) Q-factors at 15 dB OSNR (circles) and normalized insertion loss (solid line) as a function of signal wavelengths centered on the ITU grid after a concatenation of 9 × 120 km channelized FBG modules.
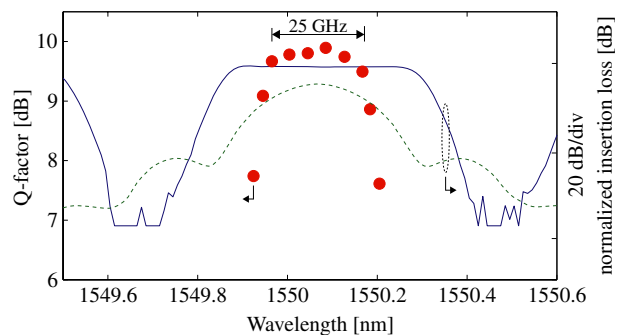

Fig. 8.   (Color online) Q-factors at 15 dB OSNR (circles) and normalized insertion loss (solid line) with respect to wavelength detuning from the ITU grid after a concatenation of 9 × 120 km channelized FBG modules, including the 112 Gbit/s DP-QPSK spectrum (dashed line).

measurements, the SMF in the link was omitted to avoid the influence of nonlinearities and the accumulated dispersion from FBG modules was compensated electronically.

In Fig. 7, Q-factors at 15 dB OSNR (circles) after a concatenation of 9 × 120 km channelized FBG modules are plotted as a function of the signal wavelengths centered on the ITU grids. The normalized insertion loss of the concatenated modules (solid line) is also included in the plot. As seen, the Q-factors are found to be approximately 9.9 dB (on average) with small variation (~0.2 dB) among the 11 probed channels. A similar Q-factor measurement was also performed with respect to wavelength detuning from the ITU grid using the same setup. The results, which are depicted in Fig. 8 (circles), show less than 0.5 dB penalty of the Q-factor when the signal wavelength is detuned within ±12.5 GHz of the center frequency. Beyond this range, however, more than 2 dB degradation of the Q-factor is observed, which is due to the module's channelization. Note that the back-to-back Q-factor at 15 dB OSNR was found to be approximately 10 dB (approximately 1 dB worse than the theoretical limit).

Figure 9 plots Q-factors at 15 dB OSNR (circles) and the averaged GDR (solid line) over a 28 GHz analysis window after a concatenation of 8 (5×120 km+3×80 km) continuous modules with respect to signal wavelengths over a 20 nm range with
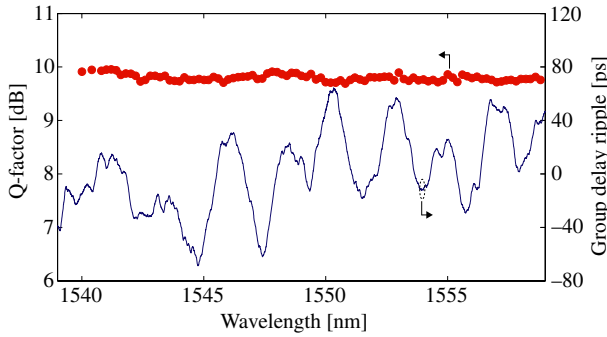
Fig. 9. (Color online) Q-factors at 15 dB OSNR (circles) and averaged GDR (solid line) as a function of signal wavelengths after a concatenation of 8 (5 × 120 km + 3 × 80 km) continuous FBG modules.
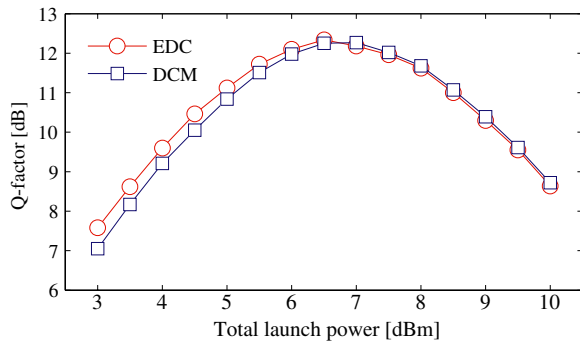

Fig. 10. (Color online) Q-factors after 840 km transmission with a 381-tap EDC (circles) and a concatenation of 8 (5 × 120 km + 3 × 80 km) continuous modules (squares) as a function of total launch power.

0.2 nm step. As seen, we notice less than 0.3 dB variation of the Q-factor regardless of the amount of GDR induced by the FBG modules across the probed wavelengths. Note that the use of mixed versions of continuous FBG modules in these experiments is due to the lack of adequate 120 km modules to achieve dispersion compensation for >800 km transmission of SMF.

Lastly, the performance comparison between the 112 Gbit/s DP-QPSK systems implementing EDC and a concatenation of 8 (5 × 120 km + 3 × 80 km) continuous modules for dispersion compensation was conducted over an 840 km straight-line SMF link. In the case of the FBG-based system, $P_{\mathrm{L,FBG}}$ was adjusted to be the same as $P_{\mathrm{L,SMF}}$, resulting in approximately 0.4 dB OSNR degradation at the receiver due to additional insertion loss imposed by the FBG modules. Figure 10 plots the Q-factors as a function of P_{L} for both systems. As seen, in linear transmission (low launch powers), the system with FBG modules provides 0.4 dB lower Q-factor, which is consistent with the OSNR degradation. However, since fiber nonlinearities are dominant at the optimal P_{L} and beyond (≥6.5 dBm), the 0.4 dB advantage found in the system with EDC vanishes. Note that the operating wavelength in this comparison was 1553.12 nm and the equalizer $N_{\mathrm{tap}} = 15$ was used.
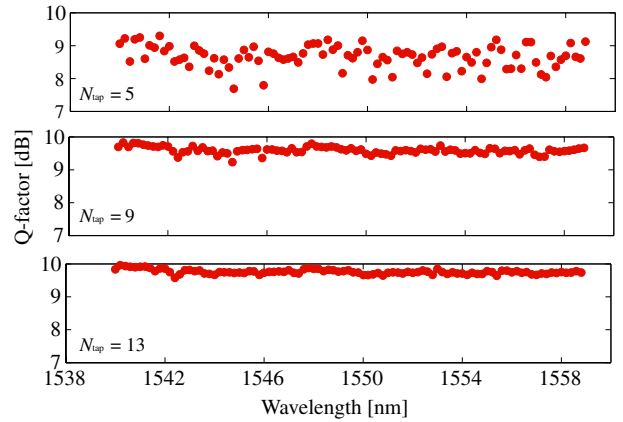

Fig. 11. (Color online) Q-factors at 15 dB OSNR as a function of signal wavelength after a concatenation of 8 (5 × 120 km + 3 × 80 km) continuous FBG modules with three different values of equalizer N_{tap}.

V. GDR MITIGATION CAPABILITY IN COHERENT-DETECTION SYSTEMS

In the preceding section, we have shown that with $N_{\mathrm{tap}} = 15$ the GDR-induced penalty is practically negligible due to the GDR mitigation capability of the linear equalizer. In this section, we further concentrate on the GDR mitigation capability in the 112 Gbit/s systems with limited equalizer N_{tap}. The mitigation capability here is quantified in the form of the Q-factor variation over the probed wavelengths. Similarly to the preceding experiments, the investigation was carried out over a concatenation of 8 (5 × 120 km + 3 × 80 km) continuous FBG modules without SMFs in the link.

Figure 11 depicts Q-factors measured at 15 dB OSNR over 20 nm with three different values of N_{tap}. As seen, larger N_{tap} provides smaller variance of the Q-factor across the probed wavelengths. This is because the FBG-induced GDR gives rise to inter-symbol interference. Hence, an adequate N_{tap} is required to effectively suppress such an impairment. To summarize the impact of the equalizer N_{tap}, in Fig. 12 we plot standard deviations (circles) and peak-to-peak variations (squares) of Q-factors across the probed wavelengths as a function of the equalizer's tap number. It is evident that at least 9 taps (corresponding to a frequency resolution of 56/9 = 6.2 GHz) are required to reduce the Q-factor variation to 1 dB after a concatenation of 8 (5 × 120 km + 3 × 80 km) continuous FBG modules.

VI. CONCLUSION

We have experimentally investigated the feasibility of implementing FBG modules for dispersion compensation in high-speed transmission systems with both differential and coherent detection and have shown the benefits of using the FBG modules in both systems.

For differential-detection systems, we have, for the first time, compared the GDR-induced penalty in 40 GBd *M*-ary RZ-DPSK (*M* = 2, 4, 8) systems and shown that this penalty increases with the signal's symbol-rate and the number of
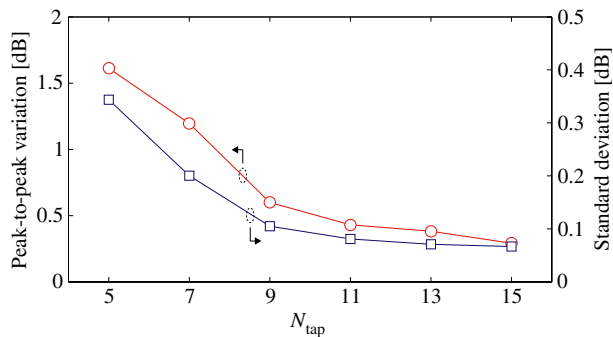
Fig. 12.   (Color online) Peak-to-peak variation (circles) and standard deviation (squares) of Q-factors as a function of the equalizer N_{tap}.

modulation levels. We have also shown that, for 5×80 Gbit/s 100-GHz-spaced RZ-DQPSK transmission over a 480 km SMF link, substituting DCFs with FBG modules results in a 2 dB higher optimal $P_{L,SMF}$, which leads to more than 3 dB OSNR improvement at the receiver. Indeed, this improvement overcomes the small GDR-induced penalty arising from a concatenation of 4×120 km continuous FBG modules.

For the 112 Gbit/s DP-QPSK coherent system, we have found that the GDR-induced impairment imposed by a concatenation of 8 (5×120 km + 3×80 km) continuous FBG modules and a concatenation of 9×120 km channelized modules is practically negligible, given that an equalizer $N_{tap} \geq 13$ is used. Furthermore, we have for the first time demonstrated that at the optimal launch power, the system using FBG modules provides a similar performance to that implementing EDC despite the fact that the former system delivers 0.4 dB lower OSNR at the receiver. Lastly, we have quantified that the dynamic equalizer's resolution must be at least 6.2 GHz to reduce the variation of Q-factors to within 1 dB. All in all, the use of FBG modules in 112 Gbit/s coherent systems allows the removal of the static equalizer, i.e., EDC, at the expense of a small increase in dynamic equalizer tap number.

Acknowledgments

References

[1] M. H. Eiselt, C. B. Clausen, and R. Tkach, "Performance characterization of components with group delay fluctuation," *IEEE Photon. Electron. Lett.*, vol. 15, no. 8, pp. 1076–1078, 2003.

[2] X. Liu, L. F. Mollenauer, and X. Wei, "Impact of group-delay ripple in transmission systems including phase-modulated formats," *IEEE Photon. Electron. Lett.*, vol. 16, no. 1, pp. 305–307, 2004.

[3] A. Dochhan, G. Göger, S. Smolorz, H. Rohde, and W. Rosenkranz, "The influence of FBG phase ripple distortions - comparison for different modulation formats," in *Optical Fiber Communication Conf. (OFC)*, Mar. 2008, JWA60.

[4] M. Filer and S. Tibuleac, "Estimation of phase ripple penalties for 40 Gb/s NRZ-DPSK transmission," in *Optical Fiber Communication Conf. (OFC)*, Mar. 2009, NWD2.

[5] J.-P. Elbers and C. Fürst, "Group-delay ripple induced performance degradation in optical DQPSK transmission," in *European Conf. in Optical Communication (ECOC)*, Mar. 2006, We3.P.107.

[6] H. Bissessur, C. Bastide, and A. Hugbart, "Performance characterization of components with phase ripple for different 40 Gb/s formats," in *Optical Fiber Communication Conf. (OFC)*, Mar. 2005, OFN4.

[7] D. van den Borne, V. Veljanovski, E. de Man, U. Gaubatz, C. Zuccaro, C. Paquet, Y. Painchaud, S. L. Jansen, E. Gottwald, G. D. Khoe, and H. de Waardt, "Cost-effective 10.7-Gbit/s long-haul transmission using fiber Bragg gratings for in-line dispersion compensation," in *Optical Fiber Communication Conf. (OFC)*, Mar. 2006, OthS5.

[8] D. van den Borne, V. Veljanovski, U. Gaubatz, C. Paquet, Y. Painchaud, E. Gottwald, G. D. Khoe, and H. de Waardt, "42.8-Gb/s RZ-DQPSK transmission with FBG-based in-line dispersion compensation," *IEEE Photon. Technol. Lett.*, vol. 19, no. 14, pp. 1069–1071, 2007.

[9] V. Veljanovski, M. Alfiad, D. van den Borne, S. L. Jansen, and T. Wuth, "Equalization of FBG-induced group-delay ripples penalties using a coherent receiver and digital signal processing," in *Optical Fiber Communication Conf. (OFC)*, Mar. 2009, JThA40.

[10] C. Xie, "WDM coherent PDM-QPSK systems with and without inline optical dispersion compensation," *Opt. Express*, vol. 17, no. 6, pp. 4815–4823, 2009.

[11] Y. K. Lizé, L. Christen, X. Wu, J.-Y. Yang, S. Nuccio, T. Wu, A. E. Willner, and R. Kashyap, "Free spectral range optimization of return-to-zero differential phase shift keyed demodulation in the presence of chromatic dispersion," *Opt. Express*, vol. 15, no. 11, pp. 6817–6822, 2007.

Ekawit Tipsuwannakul was born in Bangkok, Thailand, in 1982. He received his B.Sc. degree in electrical engineering from Chulalongkorn University, Bangkok, Thailand, in 2004, and his M.Sc. degree in photonics from the Royal Institute of Technology (KTH), Stockholm, Sweden, in 2008. He is currently working toward a Ph.D. degree at Chalmers University of Technology, Gothenburg, Sweden. During 2004–2006, he served as a Test Engineer for the Optical Transmitter/Receiver Manufacturing Group, Fabrinet Co. Ltd, Bangkok, Thailand. He later joined Svedice/Northlight AB, Stockholm, Sweden, in 2006, where he spent two years involved in system designs for high-speed optical transmitter/receiver characterizations. His research toward the Ph.D. degree is devoted to high-speed optical transmission systems using multilevel modulation formats and all-optical signal processing.

Jianqiang Li (S'05–M'10) received his B.E. degree in communications engineering and Ph.D. degree in electronics engineering from Beijing University of Posts and Telecommunications, Beijing, China, in 2005 and 2009, respectively. In July 2009, he joined Fujitsu R&D Center, Beijing, China, where he was engaged in research on digital coherent receivers for high-speed optical communication systems. Since June 2011, he has been with the Photonics Laboratory, Department of Microtechnology and Nanoscience, Chalmers University of Technology, Gothenburg, Sweden, as a postdoc researcher. His research experience and interests include high-speed and high spectral efficiency optical communication systems and microwave photonics. Dr. Li was the vice-president of the IEEE student branch at Beijing University of Posts and Telecommunications, Beijing, China, for two years. He has authored and co-authored one book in Chinese and over 40 journal and conference papers on optical transmission systems and microwave photonics.

Tobias A. Eriksson was born in Sandviken, Sweden, in 1986. He received his M.Sc. degree in electrical engineering from Chalmers University of Technology, Gothenburg, Sweden, in 2011. After graduation he joined the Photonics Laboratory at Chalmers University of Technology, where he is currently working toward a Ph.D. degree. His research focuses on various aspects of long haul fiber optical communication systems with coherent detection.

Peter A. Andrekson (S'88–SM'02–F'06) received his Ph.D. from Chalmers University of Technology, Sweden, in 1988. After about three years with AT&T Bell Laboratories, Murray Hill, NJ, USA, during 1989–1992, he returned to Chalmers where he is now a Full Professor in the Department of Microtechnology and Nanoscience. He was Director of Research at Cenix Inc. in Allentown, PA, USA, during 2000–2003 and with the newly established Center for Optical Technologies at Lehigh University, Bethlehem, PA, USA, during 2003–2004. His research interests include nearly all aspects of fiber communications such as optical amplifiers, nonlinear pulse propagation, all-optical functionalities, and very high-capacity transmission. He is co-founder of the optical test & measurement company Picosolve Inc., now part of EXFO, and Professor Andrekson is Director of EXFO Sweden AB. Professor Andrekson is a Fellow of the Optical Society of America and a Fellow of the IEEE. He is the author of about 350 scientific publications and conference papers in the area of optical communications, among which 80 were invited papers at leading international conferences and journals, including two tutorials at the Optical Fiber Communication Conference (OFC) in 2004 and 2011. He is an elected member of the Board of Governors for the IEEE Photonics Society and is or has served on several technical program committees, including OFC and ECOC, and as an international project and candidate evaluator, and has also twice served as an expert for the evaluation of the Nobel Prize in Physics. He was an associate editor for *IEEE Photonics Technology Letters* during 2003–2007. In 1993 he was awarded a prize by the Swedish government research committee for outstanding work performed by young scientists, and in 2000 he was awarded the Telenor Nordic research award for his contribution to optical technologies.

Magnus Karlsson received his Ph.D. in electromagnetic field theory in 1994 from Chalmers University of Technology, Gothenburg, Sweden. Since 1995, he has been with the Photonics Laboratory at Chalmers, first as an Assistant Professor and since 2003 as a Professor in photonics. He has authored or co-authored over 200 scientific journal and conference contributions and holds two patents. He has served on the technical committees for the Optical Fiber Communication Conference (OFC) (2009 as subcommittee chair), the Optical Amplifiers and Applications (OAA), and the Nonlinear Photonics meetings. He is currently serving on the technical program committees for the European Conference on Optical Communication (ECOC) and the Asia Communications and Photonics Conference (APC). He has served as guest editor for the *Journal of Lightwave Technology* and is an associate editor of *Optics Express*. He is a Fellow of the Optical Society of America.

His research has been devoted to a variety of aspects of fiber optic communication systems, in particular transmission effects such as fiber nonlinearities and polarization effects, but also applied issues such as high-capacity data transmission and all-optical switching. Currently he is mainly working on parametric amplification, multilevel modulation formats, and coherent transmission in optical fibers.

Lars Egnell worked with radio development for Ericsson Radio Systems from 1970 to 1976. During the 80s he held the position of Manager, Optical Communications Research at Telia, and from 1990 to 1993 he was working for Ericsson in Japan as a technical liaison officer. In 1993 Egnell founded Transport Network Application Laboratory at Ericsson, which he also managed until 1998 and where he pioneered the development of the new DWDM product family. In 1998 Egnell founded Qeyton Systems AB, where he held positions as both CEO and CTO until 2000, when the company was acquired by Cisco. Since 2001 he has been an active investor in startup companies. Egnell holds a Masters degree and a Ph.D. from the Royal Institute of Technology in Stockholm, specialized on transmission and optical communication.

Fredrik Sjöström received his M.Sc. degree in Electrical Engineering from Chalmers University of Technology, Gothenburg, Sweden, in 1998. After working in various positions at Micronic Laser Systems AB for 10 years, in the field of photomask manufacturing for semiconductors and flat panel displays, he joined Proximion in 2008. He has since been working with Technical Sales and currently holds the position of Product Manager for all fiber-Bragg-grating-based dispersion products within the company. F. Sjöström holds three patents.

Johan Pejnefors received his Ph.D. degree in solid state electronics from the Royal Institute of Technology (KTH) in Stockholm, Sweden, in 2001, and his M.Sc. degree in material physics from Uppsala University, Sweden, in 1996. He has more than 10 years of experience in research and development of optical components at FLIR and Proximion. Dr. Pejnefors has authored and co-authored more than 15 scientific papers and holds 2 patents.